Optical Boundary-Layer Transition Detection in a Transonic Wind Tunnel

M. Azzazy* and D. Modarress*
Spectron Development Laboratories, Inc., Costa Mesa, California
and
R. M. Hall†
NASA Langley Research Center, Hampton, Virginia

There are many urgent requirements for the measurement of boundary-layer transition during wind-tunnel tests. This paper highlights an instrument system based on a highly sensitive interferometer that is designed to measure the density fluctuations in compressible boundary layers. By determining the density fluctuations, the state of the boundary layer then can be inferred by the nature and level of these fluctuations. The instrument's principles of operation and description as well as recent results from a transonic test in the Boeing Model Transonic Wind Tunnel will be summarized.

I. Introduction

THERE has been a continuing need for instrumentation to measure the location of boundary-layer transition. In fact, this need is growing more acute with renewed interest in the supersonic and hypersonic flow regimes. Determining the location of transition is vital for obtaining basic experimental measurements, understanding tunnel to tunnel differences, and validating computer calculations. Determining transition in the transonic flow regime remains important for the same reasons.

Present techniques for boundary-layer transition detection generally are intrusive and model-dependent. Flow-visualization techniques such as oil sublimation[1] and smoke wire[2] can provide valuable information. Unfortunately, they usually require special preparation of the model surface, do not yield quantitative results about the transition area, and are dependent on the skills of the operator.

Thin-film techniques also have been used to detect the transition region.[3,4] However, they do require a large number of gages to be installed on the model surface in order to locate the region of transition with precision. The relatively large surface area of traditional thin-film gages limits the sensitivity of the gage to temperature spots as large as the gage and would not provide information about microscopic fluctuations. Recent developments[5] in miniature hot films may alleviate the size constraints of this technology.

Nonintrusive techniques provide a capability to detect boundary-layer transition without disturbing the flow and generally are independent of the test model. Both holography[6,7] and optical interferometry[8-10] have been used successfully to locate boundary-layer transition in supersonic wind tunnels. So far, however, the optical methods have been limited to two-dimensional and axisymmetric cases. Detection of transition over three-dimensional flow models of arbitrary shapes requires a technique that has the capability of measuring small density fluctuations in a direction perpendicular to the flow model. This requirement imposes conditions beyond the capabilities of holography.

The technique developed in this study is based on differential interferometry and is capable of detecting minute differences in the optical path on the order of a small fraction of a wavelength in a direction normal to the flow model. The technique depends on creating an infinite fringe by interfering two laser beams of opposite polarization, which reflect back from the model surface. Fluctuations in the output signal correspond to density fluctuations in the boundary layer.

In the following discussion we describe the experimental apparatus. The experimental aspects of the technique are then discussed, and the results are presented and analyzed. The results of our work then are summarized, and conclusions are stated.

II. Experimental Apparatus

Wind-Tunnel and Test Model

The test experiments were performed at the Boeing Model Transonic Wind Tunnel. The wind tunnel is of the open-circuit type, capable of delivering freestream unit Reynolds number of 1.31×10^7/m. The undisturbed flow Mach number could be varied from 0.6 to 0.9. The test section height and width were 12 and 18 cm, respectively.

A 15-cm chord NACA 66-006 airfoil was mounted between the top and bottom walls of the tunnel. Its surface was polished to 0.15 μm surface roughness. The laser beams entered the tunnel through the side wall and struck the airfoil in a direction nearly normal to its surface. Figure 1 is a schematic showing the dimensions of the model and test section.

Optical Arrangement

The optical system is illustrated in Fig. 2. A Wollaston prism W_1 was used to split a linearly polarized laser beam into two plane polarized (S and P) beams. The polarization direction of the laser beam made a 45-deg angle with the optical axis of W_1 and the Pockels cell. The two beams then were focused into the model surface. The scattered light off of the model was collected and recombined by W_1. The detection system comprised a second Wollaston prism W_2 and two detectors. The optical axis of W_2 was oriented at 45 deg to W_1, which resulted in the interference of the two beams at the detector plane. The detectors signals I_A and I_B were 180 deg

Presented as Paper 87-1430 at the AIAA 19th Fluid Dynamics, Plasma Dynamics, and Lasers Conference, Honolulu, HI, June 8-10, 1987; received Aug. 20, 1987.

*Scientist. Member AIAA.

†Scientist. Associate Fellow AIAA.

out of phase. They are given by

$$I_A = I_0[1 + V \sin\frac{2\pi}{\lambda}(\Delta p + \Delta p_v - \gamma)] \quad (1)$$

$$I_B = I_0[1 - V \sin\frac{2\pi}{\lambda}(\Delta p + \Delta p_v - \gamma)] \quad (2)$$

where I_0 is the laser power, V the fringe visibility, Δp the optical path difference due to transition, Δp_v the optical path difference due to vibrations, and γ the phase introduced by the Pockels cell.

The highest sensitivity of the system was achieved when the difference signal $I_A - I_B$, normalized by the sum $I_A + I_B$, was at the quadrature conditions, as shown in Fig. 3, such that

$$\frac{2\pi}{\lambda}(\Delta p + \Delta p_v - \gamma) = m\pi, \qquad m = 0,1,2,3 \ldots \quad (3)$$

The Pockels cell was used to compensate for the optical path difference due to vibrations and bring the system near quadrature. Therefore, the signal can be expressed as

$$S = \frac{I_A - I_B}{I_A + I_B} = V \sin 2\pi\left(\frac{\Delta p}{\lambda}\right) \quad (4)$$

A complete discussion of the optical system and its mathematical analysis was reported earlier by the authors.[11]

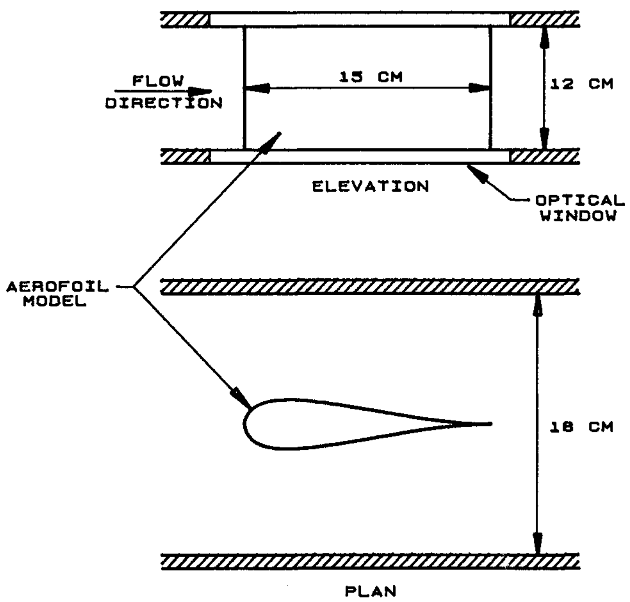

Fig. 1 Schematic of the model and test section.

Signal Processing

Figure 4 is a schematic of the signal processing system. The signal processor included signal conditioning circuits, electronic filters, and digitizers. The signal conditioning circuits obtained the difference and the sum of the two photodiode inputs $I_A - I_B$ and $I_A + I_B$ and also provided the feedback signal to the Pockels cell to achieve the quadrature condition.

The sum and the difference signals were digitized using a 5-MHz digitizer and stored on floppy disks for data evaluation. Software then was used to obtain the ratio of the difference to the sum, the rms of the ratio, and the Fourier transform of the ratio.

III. Experimental Considerations

There are a number of factors involved in the development of the boundary-layer transition detector. First, the separation of the two beams forming the interferometer arms should be greater than the characteristic length of a turbulent spot. Second, the frequency response of the system should permit the detection of the smallest turbulent spots. Finally, the system has to be capable of resolving weak phase variations so that it will be as sensitive as possible to density variations. In typical supersonic or transonic flows over a flat plate, the difference in the optical paths is of the order of $\lambda/1000$. A discussion of these factors will follow in this section.

The method of measurement is to focus the two laser beams onto the model surface and collect the backscattered light that

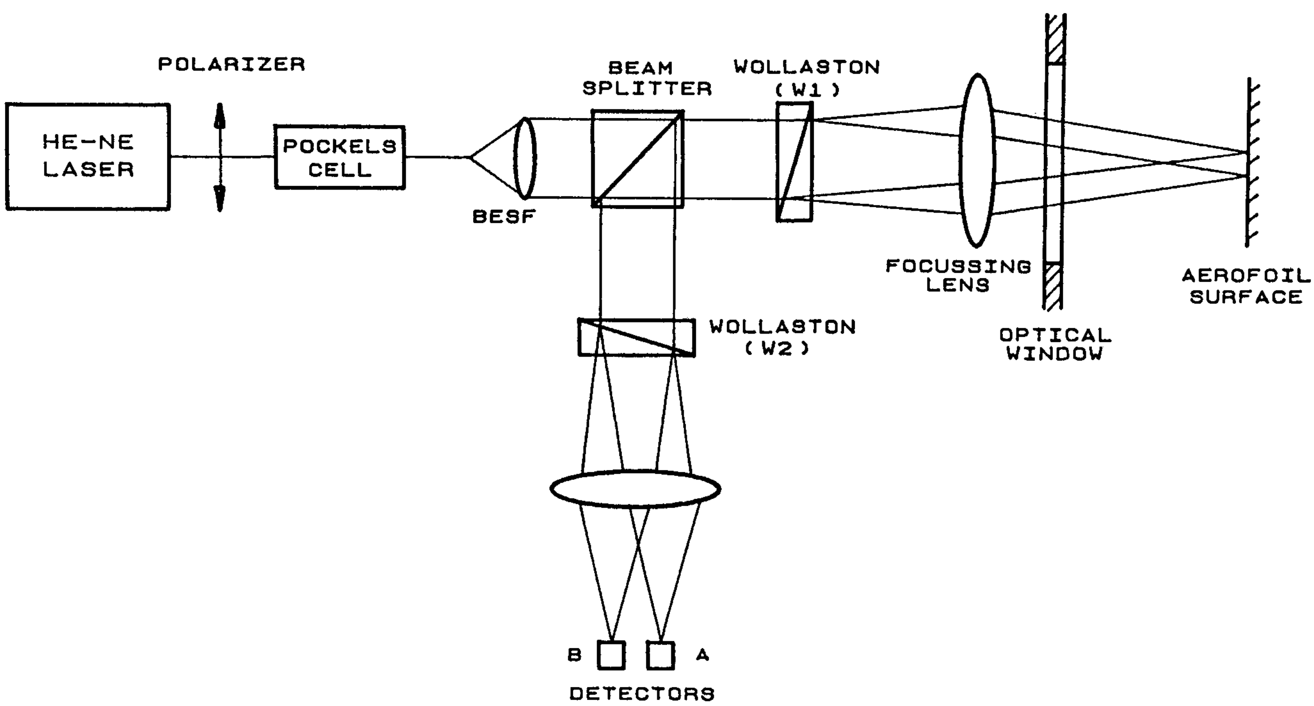

Fig. 2 Schematic diagram of the optical system.

is allowed to interfere through a Wollaston prism, W_2, as shown in Fig. 2. The two beams pass through the boundary layer on the model at different locations. Differences in density fluctuations in the boundary layer manifest themselves as optical path differences between the two beams. At the model surface the two beams were separated by 5 mm, and the electronics used for data acquisition had a bandwidth of 1 MHz and a digitization rate of 5 MHz. If the interference signal is to correspond to the passage of turbulent spots within the boundary layer, then the turbulent spot length and time scales must be reasonably less than those mentioned above. The linearized theory of laminar instability indicates that the size of a turbulent spot during transition may be characterized by an instability with a wavelength, typically five times the boundary-layer thickness.[12] In the present experiment the characteristic length scale of the turbulent spot was about 4 mm, and the interferometer beam separation was 5 mm. The hairpin eddies that form the turbulent spot fluctuate at high speeds with a typical wave speed of about twice the freestream velocity.[13] Therefore, the time scale in the present study was 7 μs, compared with 1 μs for the interferometer system. Table 1 summarizes the length and time scales of the experiment in the Boeing Model Transonic Wind Tunnel.

Table 1 Characteristic scales

	Turbulent spot	Interferometer
Time scales, μs	7	1
Length scales, mm	4	5

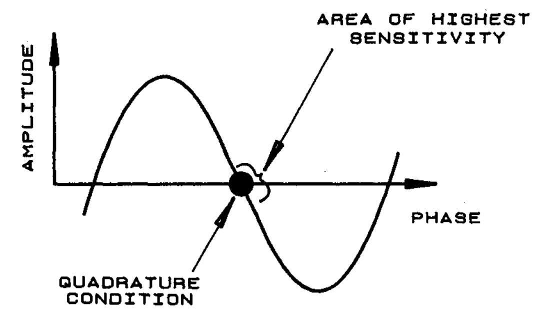

Fig. 3 Schematic of the quadrature condition.

The optical path difference Δp is related to the density fluctuations $\Delta\rho/\rho$, where ρ is the density, through the classical Dale-Gladstone constant K, such as

$$\Delta p/\lambda = (K/\lambda)(\Delta\rho/\rho)\rho\delta \tag{5}$$

where δ is the boundary-layer thickness. Theoretical predictions of boundary-layer transition show that the density fluctuations averaged over the boundary-layer thickness are about 1.5%. In typical wind-tunnel applications the boundary-layer thickness near transition is about 1 mm and the density is about 0.5 kg/m^3. Therefore, the product of the boundary-layer thickness near the transition region and the density is ~ 0.5 (mm-kg/m^3). Simple calculations show that $\Delta p/\lambda$ has to be about 0.001.

IV. Results

Experiments were performed at two freestream Mach numbers, $M = 0.7$ and 0.8, to detect both natural and roughness-induced boundary-layer transition. The interferometry technique was used to locate the transition region, and the data were verified by comparison to a fluorene sublimation technique.

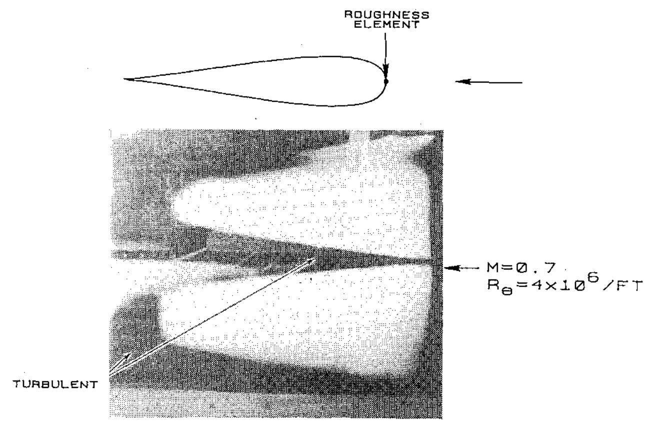

Fig. 5 Natural and tripped B. L. transition flow-visualization results.

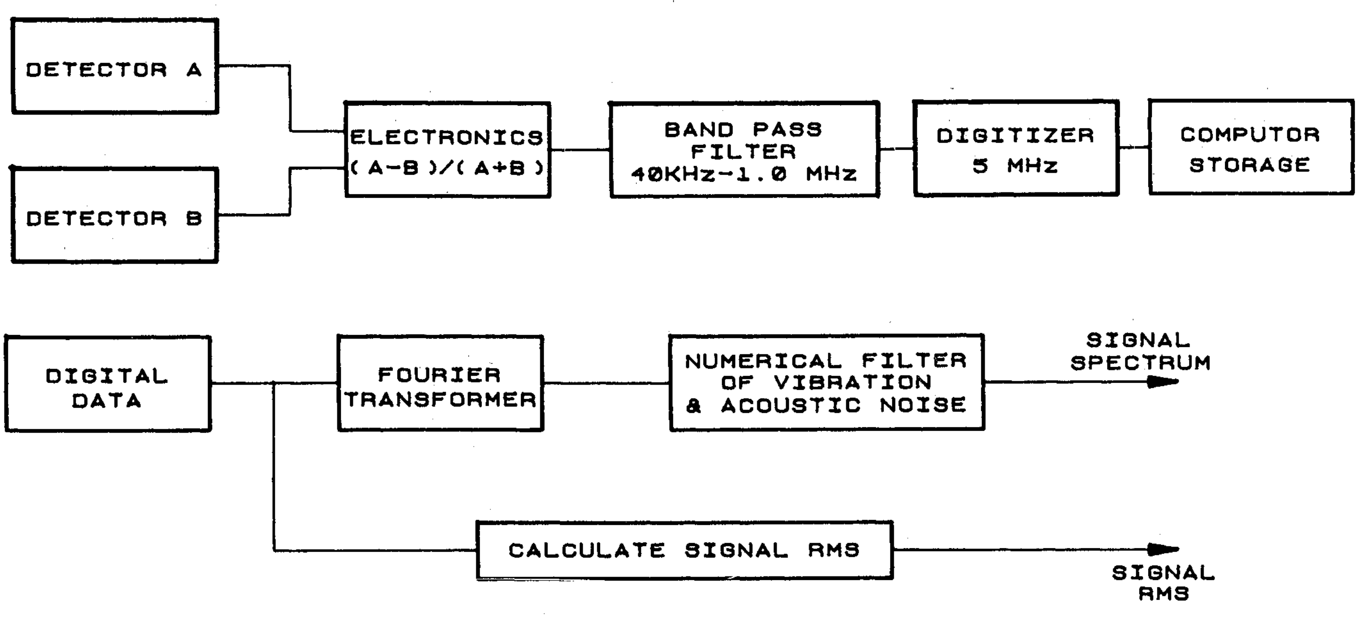

Fig. 4 Signal processing and data production.

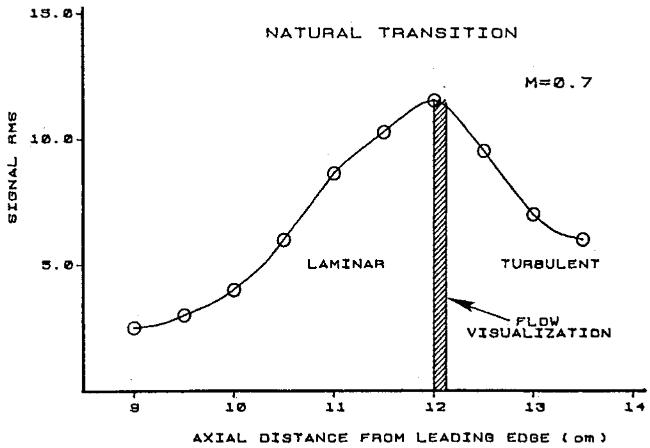

Fig. 6 Signal rms as a function of location from the leading edge during natural transition; $M = 0.7$.

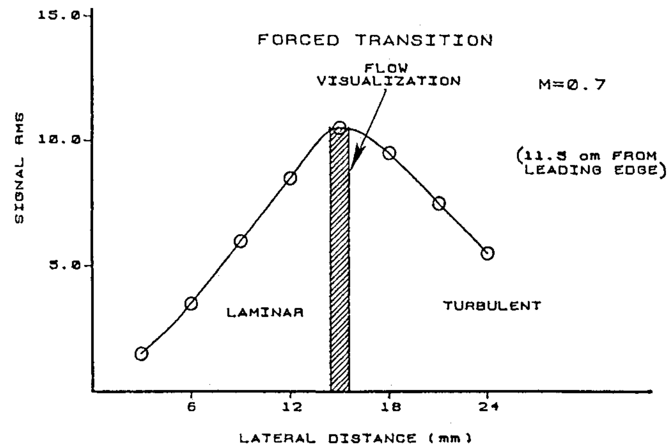

Fig. 9 Signal rms as a function of lateral distance; results are 11.5 cm from leading edge, and $M = 0.7$.

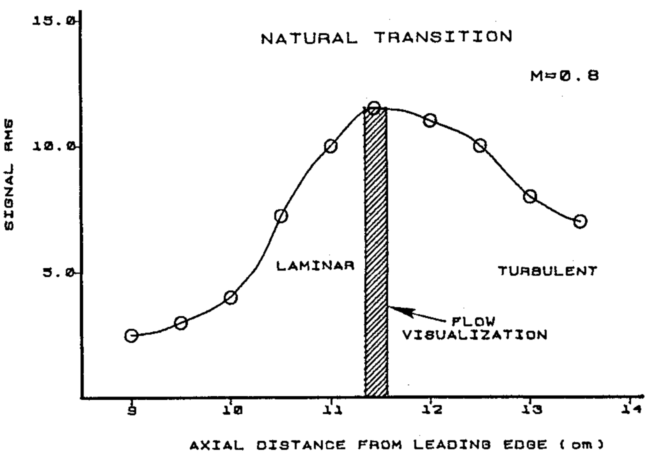

Fig. 7 Signal rms as a function of location from the leading edge during natural transition; $M = 0.8$.

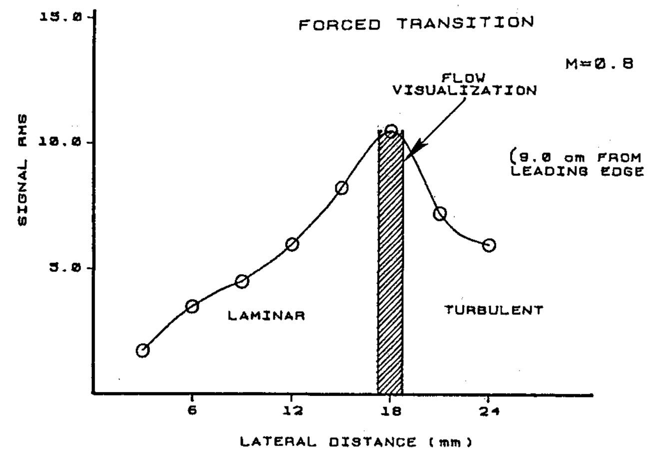

Fig. 10 Signal rms as a function of lateral distance; results are 9 cm from leading edge, and $M = 0.8$.

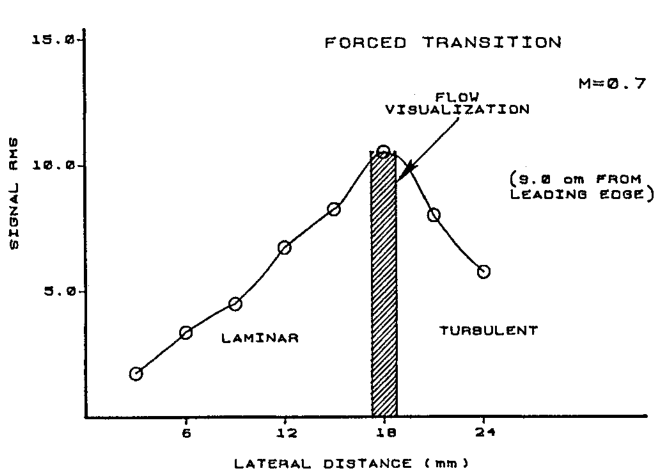

Fig. 8 Signal rms as a function of lateral distance; results are 9 cm from leading edge, and $M = 0.7$.

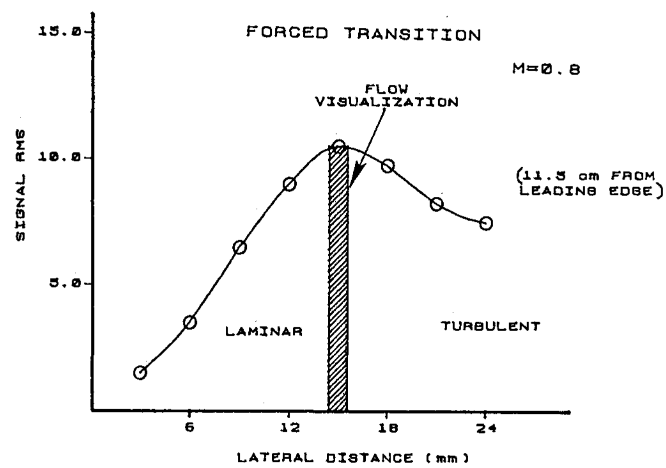

Fig. 11 Signal rms as a function of lateral distance; results are 11.5 cm from leading edge, and $M = 0.8$.

Figure 5 illustrates the type of pattern seen with the sublimating chemicals for a Mach number of 0.7 and with a roughness element attached to the leading edge of the airfoil. Several interesting features of the flow are apparent. First, a distinct turbulent wedge emanates from the leading edge as a result of the roughness element, as marked by the absence of the sublimating chemical. The absence of the whitish chemical corresponds to a region of high heat transfer, or high surface shear stress, which usually is indicative of a turbulent boundary-layer state. Second, at a location of about 5 in. from the leading edge (corresponding to the 1-in. location on the scale), it appears that natural transition is occurring that is independent of the turbulent wedges associated with either the tunnel side walls or the roughness element.

The interferometer system was used to scan the airfoil every 6 mm for natural transition and 3 mm for roughness-induced transition. Figure 6 illustrates the results for $M = 0.7$. The instrument data, shown by the circles, demonstrate an increase in signal fluctuations (indicative of density fluctuations in the boundary layer) from a region 9 cm from the leading edge rearward. This area, near 9 cm, appears to coincide with the beginning of boundary-layer transition. The unsteadiness in the signal increases until 12 cm from the leading edge, where the unsteadiness reaches a maximum and where, in fact, the line of demarcation between absence and presence of chemicals was photographically determined at an earlier time. After this peak in activity, the signal rms once again falls off as the fully turbulent region develops. However, the rms level in the fully turbulent region appears to be approaching a value of about 6 mV, compared with the laminar value of about 2 mV. Similar behavior is seen in Fig. 7 for $M = 0.8$.

Figure 8 illustrates the results for roughness-induced transition at $M = 0.7$ for a station 9 cm from the leading edge of the airfoil. Once again, signal rms is plotted on the vertical axis, whereas the spanwise position of the beams is plotted along the horizontal axis. A spanwise distance of 0 mm is actually 24 mm from the centerline of the turbulent wedge, whereas a spanwise distance of 24 mm corresponds to the centerline of the turbulent wedge. Again, the unsteadiness peak in the optical signal coincides with the boundary between the presence and absence of sublimating chemical. It is interesting that the interferometer suggests that the actual turbulent wedge generated by the roughness element is not as well defined as the sublimating chemical test suggests.

Figures 9–11 show similar results at additional Mach numbers and axial locations. In all cases, note the good agreement between the peak rms location and the sublimating chemical boundary.

The power spectrum of the digitized data was obtained numerically and normalized by the energy contained in the laminar flow. Figure 12 shows the plot of the signal power spectrum during natural transition at $M = 0.8$, at three locations: laminar, transition, and turbulence. The amount of energy contained in transition generally is higher than the laminar and turbulent regions due to the large fluctuations that usually accompany the onset of the Tollmien-Schlichting waves. The same phenomena was observed for roughness-induced transition, as shown in Fig. 13. The power spectrum

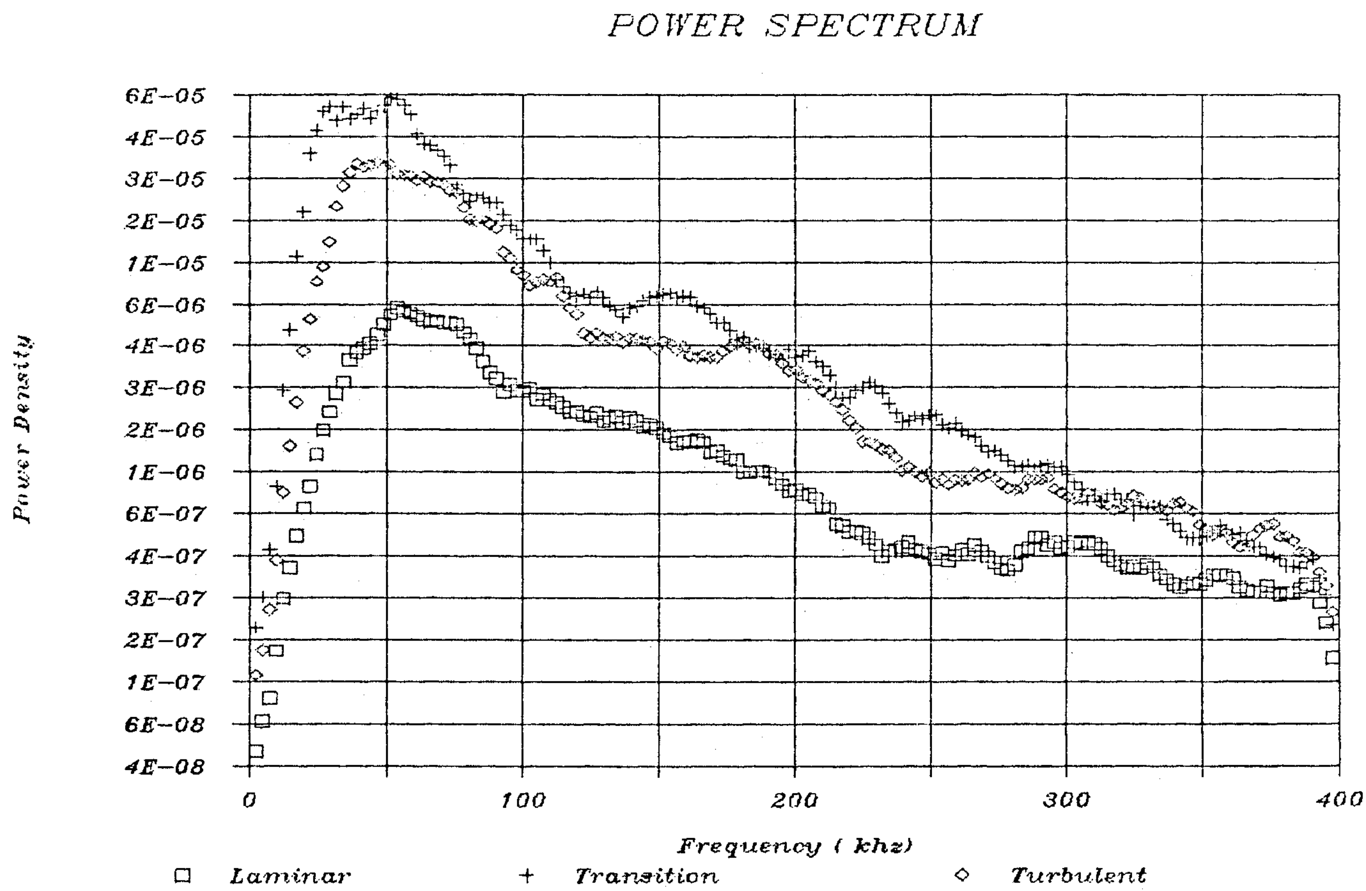

Fig. 12 Frequency spectrum during natural transition at $M = 0.8$.

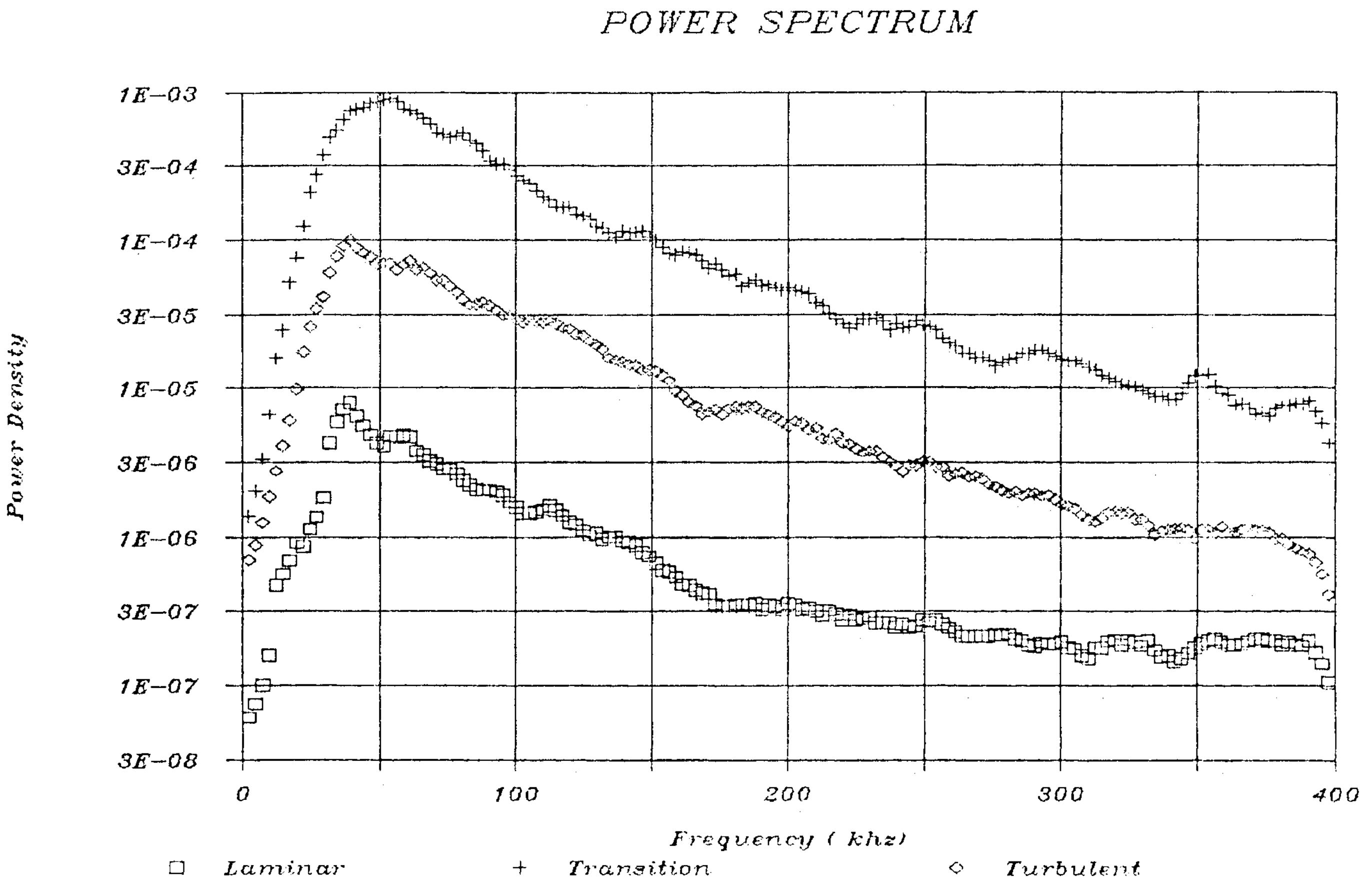

Fig. 13 Same as Fig. 12 except for turbulent wedge.

behavior, although inconclusive as an indication of transition, shows a general trend that agrees with the rms and flow-visualization results. This behavior warrants more investigation.

V. Summary and Conclusions

A high-sensitivity interferometer was developed and used to detect boundary-layer transition over a symmetric airfoil. The tests, which included both natural and roughness-induced transition, were performed in a transonic wind tunnel.

The measurements show a peak amplitude rms and higher energy in the spectrum of the signal associated with transition. The nature of the high spectrum energy at transition requires more investigation.

The test reveals that the interferometer system can be used to locate the region of transition over three-dimensional aerodynamic models.

Acknowledgments

This work was supported by NASA Langley Research Center program under Contract NAS1-18207. The authors would like to acknowledge the help of Mr. James Crowder of Boeing Commercial Air Company for providing the wind-tunnel facility and support during the experimental testing of the instrument and Dr. Hung Tan of Spectron for providing the data processing software.

References

[1]Cassels, W. A. and Campbell, J. F., "Boundary-Layer Transition Study of Several Pointed Bodies of Revolution at Supersonic Speeds," NASA TN D-6063, 1970.

[2]Batill, S. M. and Mueller, T. J., "Visualization of Transition in the Flow Over an Airfoil Using the Smoke-Wire Technique," *AIAA Journal,* Vol. 19, March 1981, pp. 340–345.

[3]Fancher, M. F., "Aspects of Cryogenics Wind Tunnel Testing Technology at Douglas," AIAA Paper 82-0606, Jan. 1982.

[4]Stallings, R. L., Jr. and Lamb, M., "Effects of Roughness Size on the Position of Boundary-Layer Transition and on the Aerodynamic Characteristics of a 44° Swept Delta Wing at Supersonic Speeds," NASA TP-1027, 1977.

[5]Johnson, C. B., Carraway, D. L., Stainback, P. C., and Fancher, M. F., "A Transition Detection Study Using a Cryogenic Hot Film System in the Langley 0.3-Meter Transonic Cryogenic Tunnel," AIAA Paper 87-0049, Jan. 1987.

[6]Havener, A. G., "Detection of Boundary-Layer Transition Using Holography," *AIAA Journal,* Vol. 15, April 1977, pp. 592–293.

[7]Hanever, A. G., "Holographic Measurement of Transition and Turbulent Bursting in Supersonic Axisymmetric Boundary Layers," AIAA Paper 83-1724, June 1983.

[8]Laderman, A. J. and Demetriades, A., "Detection of Boundary-Layer Transition with a Laser Beam," *AIAA Journal,* Vol. 14, Jan. 1976, pp. 102–104.

[9]Smeets, G., "A High Sensitivity Laser Interferometer for Transient Phase Objects," Proceedings of the 8th International Shock Tube Symposium, London, 1971, pp. 45/1–45/10.

[10]Smeets, G. and George A., "Investigation of Shock Boundary Layers with a Laser Interferometer," Proceedings of the 9th International Shock Tube Symposium, Stanford Univ. Press, Stanford, CA, July 1983, pp. 429–438.

[11]Azzazy, M., Modarress, D., and Hoeft, T., "High Sensitivity Density Fluctuation Detector," *Journal of Physics: E: Scientific Instruments,* Vol. 20, 1987, pp. 428–431.

[12]Maslowe, S. A., "Shear Flow Instabilities and Transition," *Topics in Applied Physics: Hydrodynamic Instabilities and the Transition to Turbulence,* Vol. 45, edited by H. L. Swinney and J. P. Gollub, Springer-Verlag, New York, 1981, Chap. 7.

[13]Gad-El-Hak, M., Blackwelder, R. F., and Riley J., "On the Growth of Turbulent Regions in Laminar Boundary Layers," *Journal of Fluid Mechanics,* Vol. 110, 1981, pp. 73–95.